https://www.cytojournal.com/

CytoJournal

Editor-in-Chief:
Miaoqing Zhao, PhD., MD (Shandong First Medical University, Jinan, China)
He Wang, MD, PhD (Yale University School of Medicine, New Haven, Connecticut, USA)
Founding Editor & Editor-in-chief Emeritus:
Vinod B. Shidham, MD, FIAC, FRCPath (WSU School of Medicine, Detroit, USA)

OPEN ACCESS

Research Article

Influence of sodium ferulate on neutrophil extracellular traps-platelet activation-mediated endothelial dysfunction in immune small vasculitis

Xiaoli Zhou, MD[1,#], Zhuojun Wang, MM[1,#], Weixiang Liao, MM[1], Qianlu Yin, MM[2], Chuan Xiong, MM[2], Yuhang Zheng, MM[2], Wei Peng, MBBS[1]

[1]Department of Peripheral Vascular (Wound Repair), Chongqing Traditional Chinese Medicine Hospital, Chongqing, [2]Graduate School, Guizhou University of Traditional Chinese Medicine, Guiyang, China.
[#]The authors shared the first authorship.

***Corresponding author:**
Xiaoli Zhou,
Department of Peripheral Vascular (Wound Repair), Chongqing Traditional Chinese Medicine Hospital, Chongqing, China.

tiny1976@163.com

Received: 09 August 2024
Accepted: 06 November 2024
Published: 27 December 2024

DOI
10.25259/Cytojournal_153_2024

Quick Response Code:

ABSTRACT

Objective: Anti-neutrophil cytoplasmic antibody (ANCA)-associated vasculitis (AAV) is an autoimmune disease that is challenging to treat. This study aimed to identify the effect of sodium ferulate on endothelial dysfunction mediated by neutrophil extracellular trap (NET)–platelet activation in AAV to provide potential strategies for AAV treatment.

Material and Methods: An animal model of myeloperoxidase (MPO)-AAV passive immune vasculitis was established using anti-MPO immunoglobulin G and Rag2 knockout mice. The efficacy and mechanism of action of sodium ferulate in AAV were explored in cultured and isolated endothelial progenitor cells (EPCs), and messenger ribonucleic acid gene expression, relative protein expression, and protein fluorescence intensity were determined through quantitative polymerase chain reaction, Western blotting, and immunofluorescence, respectively. Serum antibody concentrations were determined by enzyme-linked immunosorbent assay, and flow cytometry was used in determining the expression levels of platelet-selectin (CD62p) and procaspase-activating compound-1 (PAC-1) on the surfaces of the platelets. The EPCs' ultramicroscopic structure was observed through transmission electron microscopy.

Results: The expression levels of ANCA, histone H3 citrullinated, and MPO protein fluorescence intensity in MPO-AAV mice were inhibited by sodium ferulate, and the expression levels of CD62p and PAC-1 on the cell surface were reduced. The relative expression levels of β-trace protein (β-TG), soluble thrombomodulin, inducible nitric oxide synthase (iNOS), and tumor necrosis factor α decreased. We found that sodium ferulate inhibited NETs' free DNA and mitigated damage in EPCs. In addition, relative expression levels of von Willebrand Factor, β-TG, and iNOS and serum concentrations of PAC-1, β-TG, and iNOS were inhibited.

Conclusion: Sodium ferulate can treat AAV by inhibiting NET release and platelet activation and reducing endothelial cell damage.

Keywords: antineutrophil cytoplasmic antibody, vasculitis, sodium ferulate, neutrophil extracellular trap, platelet

INTRODUCTION

Manifested as inflammation and fibrinoid necrosis within the walls of small blood vessels, antineutrophil cytoplasmic antibody (ANCA)-associated vasculitis (AAV) is a systemic

autoimmune disorder. This condition arises owing to the malfunction of the immune system, leading to an erroneous attack on the body's own healthy cells and tissues. It frequently engages small-scale blood pathways and affects the kidneys, showcasing itself through injury to the glomerular vasculature, fibrinoid necrosis, and infrequent accumulation of immune complexes. The disease rapidly progresses and has poor prognosis.[1] Clinical presentations, imaging results, pathological findings, serological analyses, and other distinguishing attributes show that AAV primarily encompasses eosinophilic granulomatosis with polyangiitis, polyangiitis, and microscopic polyangiitis.[2] In the serum samples of individuals with AAV, ANCA is directed against either target antigen proteinase 3 (PR3) or myeloperoxidase (MPO). Thus, AAV is categorized as PR3-ANCA and MPO-ANCA. Differentiation leads to differences in the levels of kidney engagement, affected organs, lesion types, and eventual prognoses. ANCA is the first autoantibody confirmed to be associated with vasculitis[3] and is considered an important indicator for the diagnosis and monitoring of AAV activity.[3]

Neutrophil extracellular traps (NETs) are structures released by neutrophils and contain DNA and antimicrobial proteins that effectively trap and neutralize bacteria, fungi, parasites, or viruses and are involved in inflammatory responses.[4,5] NETs play a beneficial role in the management of bacterial infections.[6] Patients with sepsis exhibit elevated levels of circulating NETs possibly because of the diminished clearance of NET-released products. Cell-free DNA intensifies an inflammatory response by inducing tumor necrosis factor α (TNF-α) messenger ribonucleic acid (RNA) expression.[7] In addition, histones serve as damage-associated molecular patterns that can result in organ damage by promoting the release of pro-inflammatory cytokines and causing endothelial dysfunction through the induction of cytotoxicity and increase in reactive oxygen species production.[8] Furthermore, NETs are associated with pathological alterations in autoimmune and autoinflammatory diseases,[9] including psoriasis,[10] systemic lupus erythematosus,[11] rheumatoid arthritis,[12] small-vessel vasculitis,[13] and inflammatory bowel diseases.[14]

AAV treatment progresses through three distinct phases: Initiation of remission, upholding remission, and relapse.[15] The induction period of remission is key to the clinical treatment of AAV, and the treatment effect often directly affects the prognoses of patients.[16] To date, hormones combined with immunosuppressive agents are often used to treat AAV. However, these treatment regimens are prone to induce toxic side effects, cause major stress, and cause co-infection. Hence, exploring novel therapeutic approaches is crucial for extending the progression of the illness.

Sodium ferulate, a natural phenolic acid, is the main component of traditional Chinese medicines for promoting blood circulation and removing blood stasis, such as *Angelica sinensis* and *Ligusticum chuanxiong*. It has anti-apoptotic, antiplatelet aggregation, and antithrombotic effects.[17] Sodium ferulate can protect human umbilical vein endothelial cells damaged by oxidized low-density lipoprotein by downregulating the expression of the chemokine ligand 1 gene.[18] In the application of clinical treatment, sodium ferulate is mostly used as an adjuvant therapy for vascular diseases such as atherosclerosis and coronary heart disease.[19] However, regarding the crucial question of whether it can play a positive role in alleviating vasculitis, there has been no in-depth research and no definite conclusion so far.

In this experiment, anti-MPO immunoglobulin G (IgG) was passively transferred to Rag2 knockout (KO) mice to establish a passive immunization mouse model of MPO-AAV, and the therapeutic effect of sodium ferulate on MPO-AAV mice was tested. In addition, endothelial progenitor cells (EPCs) isolated from peripheral blood mononuclear cells (PBMCs) of AAV patients were treated with sodium ferulate, and the effects of sodium ferulate on AAV NETs, platelet activation, and endothelial dysfunction were investigated at the cellular level. This research explores the use of sodium ferulate in AAV treatment by exploring the efficacy of sodium ferulate and provides an alternative therapy for AAV treatment.

MATERIAL AND METHODS

Consent to participate

Informed consent was obtained from all participants for all experiments in this study after the nature and potential risks of the study were explained to them. They were also informed of their right to withdraw from the study at any time without penalty.

Animal model of MPO-AAV

This study followed the management methods for laboratory animals that were approved by the Ethics Committee of Chongqing Traditional Chinese Medicine Hospital (Approval No. 2022-DWSY-ZXL; Approval Date: November 7, 2022). Fifteen $Rag2^{-/-}$ mice (7–8 weeks, specific pathogen - free grade) were purchased from Chongqing Ensiweier Biotechnology Co., Ltd. The indoor temperature of the rearing room was 22°C ± 2°C, humidity was 60%, day and night alternated for 12 h, and the rats were provided with fresh and nutritionally balanced feed and clean water throughout the experimental period. The rats received fresh and nutritionally balanced feed and clean water throughout the experimental period and were subjected to regular health checkups so that health problems can be detected and addressed promptly. An animal model of immune small vasculitis was established by transferring anti-MPO IgG (GTX11730, Gene Tex, California, America)

to Recombination activating gene 2 knockout (Rag2 KO) mice.[20] During and after modeling, the general state of the mice was observed, including mobility, diet, and hair condition. MPO-AAV model mice were assessed for ANCA expression via immunofluorescence staining to validate successful model construction. The sodium ferulate group was administered by intraperitoneal injection (100 mg/kg, continuously for 10 days), and the control and MPO-AAV model groups received the same doses of the solvent by gavage. After 6 weeks, in the MPO-AAV mouse model, anesthesia was performed with the intraperitoneal injection of 3% pentobarbital (dose: 30 mg/kg; P3761, BSZH, Beijing, China). After successful anesthesia administration, kidney, lung, and whole blood samples were collected. Subsequently, when the mice were in a state of deep anesthesia, a 15% pentobarbital sodium solution (dose: 150 mg/kg) was slowly injected into the lateral abdominal vein, and the gradual disappearance of the vital signs of the mice was observed.

EPC culture and grouping

PBMCs were obtained from 30 *patient*s with immune vasculitis by density gradient centrifugation. All experiments involving human patients in our study followed the ethical regulations of the Ethics Committee of Chongqing Traditional Chinese Medicine Hospital and have been approved by the Committee (Ethics Approval No. 2020-ky-64, Chongqing Hospital of Traditional Chinese Medicine; Approval Date: January 25, 2021). The ethical principles set forth in the Declaration of Helsinki were duly considered throughout the process. In summary, anticoagulated whole blood was combined with an equivalent amount of phosphate-buffered saline (PBS) after dilution and thorough mixing. A centrifuge tube was loaded with 15 mL of Ficoll separation solution. Subsequently, we introduced 15 mL of thinned blood gently and gradually onto the surface of the separation solution to ensure that the interface between the two liquid surfaces remained unobscured. The mixture was centrifuged at room temperature, specifically at 1000 × g for 30 min. A white film layer, situated between the upper plasma layer and intermediate transparent separation liquid layer, constituted the lymphocyte layer. The bottom of the centrifuge tube contained red blood cells and granulocytes. Cells from the white film layer (lymphocyte layer) between the upper plasma layer and intermediate transparent separation liquid layer were carefully aspirated into a fresh centrifuge tube. The cells were then washed with 10 mL of PBS. Then, centrifugation was performed at ×250 *g* for 10 min, resulting in cellular precipitation. Subsequently, the cells were resuspended in 5 mL of PBS and centrifuged again at ×250 *g* for 10 min. After the addition of PBS and resuspension, a final centrifugation step was performed for PBMC collection. Harvested PBMCs were resuspended in endothelial basal medium-2 BulletKit medium (CC-3156, Lonza, Visp, Valais, Switzerland) supplemented with 1% penicillin and streptomycin (C0009, Beyotime, Shanghai, China) and then inoculated into culture flasks for incubation. The cells were cultured for 4 days in a 37°C incubator with 5% carbon dioxide (CO_2). After 4 days, non-adherent cells were removed by rinsing with PBS, the culture medium was replaced, and incubation was incubated until the 10th day. Adherent cells were collected after rinsing the culture flasks with PBS, followed by centrifugation. The five groups were separated from EPCs: Control (peripheral blood serum of healthy people), model (peripheral blood serum of patients with immune vasculitis), L-sodium ferulate (100 ng/mL), M-sodium ferulate (200 ng/mL), and H-sodium ferulate (400 ng/mL), and) and cultured at 37°C under 5% CO_2 for 24 h.

Cell identification of EPCs

The EPC cells were inoculated with 2 × 10^6/mL–3 × 10^6/mL in fibronectin-coated 24- and 6-well plates, collected on the 4th day of culture, and incubated with 2.4 ng/mL DiI-AC-LDL (H7970, Solarbio, Beijing, China) at 37℃ for 1 h. The cells were fixed with 2% paraformaldehyde for 10 min and washed with PBS for 2 min, and 10 ng/mL Ulex Europaeus Agglutinin I (L9006-1MG, MERCK, Darmstadt, Hesse, Germany) was added to the above specimens. The cells were incubated at 37℃ for 1 h. Cells in each well were counted with an inverted fluorescence microscope (BLD-200, KEYENCE, Osaka, Japan) in 15 randomly selected microscopic fields of view (×400), and the cells were identified through flow cytometry (CytoFLEX, Beckman Coulter, Brea, California, America) and detected for cell surface markers.

Mycoplasma testing

Mycoplasma detection in EPCs in 30 patients with immune vasculitis was performed using a Mycoplasma capsulatum enzyme-linked immunosorbent assay (ELISA) kit (CB12541-Hu, COIBO BIO, Shanghai, China). The specific operation was as follows: Standard and sample wells were set up, 50 μL of different concentrations of standards was added to each standard well, and 50 mL of the samples to be tested was added to the sample wells; the blank wells were not added. In addition to the blank wells, 100 L of horseradish peroxidase-labeled detection antibody was added to each well of the standard and sample wells. The reaction wells were sealed with a sealing film and incubated for 60 min at 37℃ in a water bath or a thermostat, the liquid was discarded, the wells were dried on blotting paper, and a full washing solution (350 μL) was added to each well. The reaction wells were left to stand for 1 min, the washing solution was shaken off, and the samples were pat-dried on the blotting paper. Plate washing was performed 5 times (a plate washer was used in washing the plates). Substrates A and B (50 μL) were added to each

well and incubated at 37°C for 15 min, 50 uL of termination solution was added to each well, and the optical density value of each well was measured at 450 nm within 15 min.

Immunofluorescence

Paraffin-embedded tissues were cut into 3 μm-thick sections with a slicer (RM2235, Leica, Wetzlar, Germany) and then dewaxed in xylene for 5 min 3 times. Antigen retrieval was performed using 10 mM sodium citrate at pH 6.0 and 95°C for 12 min in a toaster (HI1220, Leica, Wetzlar, Germany). The tissue was blocked overnight with an immunostaining blocking solution (C0265, Beyotime, Shanghai, China). The blocking solution was blotted with absorbent paper. Diluted primary antibodies (1: 200) of ANCA (ab103768, Abcam, Cambridge, United Kingdom), histone H3 citrullinated (H3Cit; 9701, Cell Signaling, Danvers, Massachusetts, America), and MPO (ab9090, Abcam, Cambridge, United Kingdom) were added dropwise, and the samples were left in a wet box at 4°C overnight. After the wet box was rewarmed, the sections were rinsed saturated with PBS 3 times for 3 min each time. Diluted fluorescent secondary antibody (1:100) (A11029, Invitrogen, Carlsbad, California, America) was incubated in a humidified box (37°C, 60 min). 2-(4-Amidinophenyl)-6-indolecarbamidine dihydrochloride (C1005, Beyotime, Shanghai, China) was added dropwise to stain the nucleus, and the samples were left to stand for 15 min in the dark. A tissue autofluorescence quencher was added, and incubation was performed for 5 min in the dark. The slides were mounted with an autofluorescence quencher (G1221, Servicebio, Wuhan, China). Observations were initially performed using an upright fluorescence microscopy system (Guangzhou Mshot Photoelectric Technology Co., Ltd.) at low magnification. Subsequently, images were acquired at ×400 magnification. ImageJ software (Fiji, National Institutes of Health, America; download site: https://imagej.net/ij/download.html) was used to merge and quantify the experimental results.

Flow cytometry

After the collected blood samples were gently mixed (this step prevented *in vitro* platelet activation due to human manipulation), 5 μL of whole blood was promptly added to a preprepared sample tube containing the monoclonal antibody. Then, 20 μL of CD61-PerCP (46–0619–42, Invitrogen, Carlsbad, California, America) was added to each sample. For the experimental tubes, 20 μL of human procaspase-activating compound-1 (PAC-1) FITC (MA5-28564, Invitrogen, Carlsbad, California, America) and CD62P (P-Selectin) Monoclonal Antibody (AK-4), PE, eBioscience™ (12-0628-42, Invitrogen, Carlsbad, California, America) were added. The reaction was performed in an environment away from light at 25°C for 20 min. For sample fixation, 1 mL of PBS containing 1% paraformaldehyde (DF0135, Leagene, Beijing, China) was added to each tube, and the tubes were incubated for 20 min. The assay was performed using a CytoFLEX flow cytometer (Beckman Coulter, Brea, California, America) within 24 h and the results of the experiments were analyzed with FlowJo X software (v10.8, BD Biosciences, America, download site: https://www.bdbiosciences.com/zh-cn/products/software/flowjo-v10-software).

Platelet thrombin generation time assay

Platelet thromboplastin generation time test was carried out using a thromboplastin time test kit (YS0335, Yaji, Shanghai, China), and the detailed procedure was carried out according to its instruction. Specifically, 1.8 mL of fresh venous blood to be tested was mixed with 0.2 mL of sodium citrate anticoagulant (109 mM) in a 9:1 ratio. The mixture was gently inverted and mixed. Centrifugation was performed at 3000 rpm (or ×2500 g) for 10–15 min, and the upper layer of the liquid (plasma lacking platelets) was transferred to a plastic tube or centrifugal tube. Normal control plasma was maintained. Anticoagulated plasma (0.1 mL) was collected and placed in a 37°C water bath and warm for 5 min. Thrombin solution (0.1 mL) was added. Coagulation time was recorded 2 or 3 times, and the average was obtained.

ELISA

The whole blood specimen collected in the serum separation tube was placed at room temperature for 2 h, and then, serum samples were acquired by centrifugation (×1000 g for 20 min). ELISA was performed in accordance with the manufacturer's instructions. The following ELISA kits were used: Platelet activating factor (PAF) (CEA526Ge, Cloud-clone Corp, Houston, Texas, America), β-TG (TW10534, Tongwei, Shanghai, China), PAC-1 (RX101227H, Ruixin BioTech, Quanzhou, China), and human inducible nitric oxide synthase (iNOS) (TW7992, Tongwei, Shanghai, China).

Western blotting

Protein (500 μg) was combined with ×5 sodium dodecyl sulfate loading buffer in a 4:1 ratio, and the final protein concentration was approximately 3.3 μg/μL. Subsequently, proteins were denatured by boiling in water at 100°C for 6 min. For loading purposes, 60 μg of denatured total protein was separated by electrophoresis at 80 V to separate the proteins. The proteins were then transferred to a polyvinylidene fluoride membrane at a constant current of 250 mA. Afterward, the membrane was washed with tris buffered saline with Tween 20 (TBST) for 1 min and blocked

with 5% skim milk at room temperature for 60 min. After blocking, the membrane was rinsed 3 times with TBST for 5 min each. Primary antibody (1:1000) was added and incubated overnight at 4°C. After incubation, the membrane was washed 3 times with TBST for 10 min each for the removal of excess primary antibodies. The membrane was then incubated with secondary antibody (1:2000; AS014, ABclonal, Wuhan, China) for 60 min and washed with TBST for 10 min 3 times. A mixture of solutions A and B from the ECL exposure aqueous solution (34580, Thermo, Waltham, Massachusetts, America) in a 1:1 ratio was applied to the membrane. After reacting for 1 min, the membrane was placed in a gel imaging system (Bio-Rad, Universal Hood II, America) for exposure detection. Finally, the trimming result images were analyzed with Image J software. All primary antibodies were purchased from ABclonal Technology Co., Ltd.: PAC-1 (A10011, ABclonal, Wuhan, China); β-trace protein (β-TG; A1925, ABclonal, Wuhan, China); soluble thrombomodulin (sTM) (A12357, ABclonal, Wuhan, China); iNOS (A0312, ABclonal, Wuhan, China); TNF-α (A11534, ABclonal, Wuhan, China); von Willebrand Factor (vWF; A13523, ABclonal, Wuhan, China); and β-actin (AC026, ABclonal, Wuhan, China).

Real-time quantitative polymerase chain reaction (qPCR)

First, RNA was retrieved from the tissues using RNAiso Plus (9108, Takara, Kusatsu, Japan) after tissue grinding. Then, using a Goldenstar RT6 complementary deoxyribonucleic acid (cDNA) Synthesis Kit Version 2 (TSK302M, Tsingke, Beijing, China), we acquired cDNA through reverse transcription using RNA as a template. The qPCR experiment was implemented according to the directions of the ChamQ Universal SYBR qPCR Master Mix kit (TSE002, Tsingke, Beijing, China) after cDNA was acquired. Experimental data were calculated using the $2^{-\Delta\Delta Ct}$ method, with the endogenous gene *GAPDH* serving as the reference point. The primer sequences used in this study are listed in Table 1.

Table 1: Primer sequences used in qPCR.

Primer name	Sequences
PAC-1-F	TTGACTGACTCCTGGGGGAA
PAC-1-R	CACCATATCAGAGCAGCCGT
β-TG-F	CCTGGCGTCAAGAGAATCGT
β-TG-R	CTTGGCTTGCCCGTCTTCAT
sTM-F	ACACAGGTAGACACACCCCAGATAG
sTM-R	CAAAAGCCATAGCCAGCAAGC
iNOS-F	CCTTGTTCAGCTACGCCTTC
iNOS-R	CTGAGGGCTCTGTTGAGGTC
TNF-α-F	CGAGTGACAAGCCCGTAGCC
TNF-α-R	GGATGAACACGCCAGTCGCC
GAPDH-F	AGGTCGGTGTGAACGGATTTG
GAPDH-R	TGTAGACCATGTAGTTGAGGTCA

qPCR: Quantitative polymerase chain reaction, PAC-1: Procaspase-activating compound-1, β-TG: β-trace protein, sTM: Soluble thrombomodulin, iNOS: Inducible nitric oxide synthase, TNF-α: Tumor necrosis factor α, GADPH: Glyceraldehyde-3-phosphate dehydrogenase, F: Forward primer, R: Reverse primer, A: Adenine, C: Cytosine, G: Guanine, T: Thymine

Detection of NETs

The procedures followed the guidelines of the PicoGreen double-stranded DNA quantitative detection kit (P9740, Solarbio, Beijing, China). Initially, a standard working solution with 1 mg/mL calf thymidine DNA dry powder (D8515, Sigma-Aldrich, St. Louis, Missouri, America) and PicoGreen dye working solution was prepared. Subsequently, 1 mg/mL calf thymine DNA dry powder standard working solution was diluted twice. A fluorometer (UV752, Yoke, Shanghai, China) was used in measuring the fluorescence values of the samples. Excitation was performed at 488 nm, and emission was detected at 520 nm. The NET concentration was determined by plotting the working curve of the standard product and measuring the sample.

3-(4,5-Dimethylthiazol-2-yl)-2,5-diphenyltetrazolium bromide (MTT) assay

EPCs were seeded in 96-well plates at a density of 200 μL/well, and three replicates were performed for each group. Cells were cultivated at 37°C and 5% CO_2 and grouped according to the above cell model after they were adhered. In each group, the samples were added and incubated for 24 h. Subsequently, 20 μL of 5 mg/mL MTT solution (M1020, Solarbio, Beijing, China) was added to each well to initiate a reaction with succinate dehydrogenase. Afterward, 4 h of incubation was carried out, the culture was then terminated, and the medium in the well was gently discarded. After the low-speed shaking of the plates for 10 min, 150 μL of dimethyl sulfoxide was added. The absorbance of each well was measured at 490 nm wavelength with a microplate reader (840–317500, NanoDrop One/One^{C}, Thermo, Waltham, Massachusetts, America).

Ultrastructural detection of EPCs

Cells were obtained by centrifugation at 1500 rpm for 10 min after digestion with trypsin. Next, a 0.5% glutaraldehyde fixative solution was added to the cells and incubated at 4°C for 10 min. For cell collection, centrifugation was performed at 10,000 rpm for 15 min, and then, 3% glutaraldehyde fixative was added slowly. Re-fixation was continued with 1% osmium tetroxide (GP18456, Leica, Wetzlar, Germany), and progressive

dehydration was performed using pyruvic acid. The dehydrated sample was successively treated with a dehydrating agent and epoxy resin infiltrate (GP18010, Zhongjingkeyi, Beijing, China) to preserve the cellular microstructure. The immersed sample block was placed in a suitable mold, filled with an embedding solution, embedded, and heated to form a solid matrix. Ultrathin slices of approximately 50 nm thick were prepared using an ultramicrotome (EMUC7, Leica, Wetzlar, Germany), floated on the liquid surface of the knife bath, and then applied onto a copper mesh. The sections were stained with uranyl acetate (GS02624, Zhongjingkeyi, Beijing, China) for 10–15 min at 25°C and then with lead citrate (GZ02616, Zhongjingkeyi, Beijing, China) for 1–2 min and photographed with a transmission electron microscope (JEM-1400PLUS, JEOL, Akishima, Tokyo, Japan).

Statistical analysis

The collected data were analyzed using GraphPad Prism 8.0.1 (8.0.1, GraphPad Software, America, download site: https://www.graphpad-prism.cn) software, and the outcomes were depicted as mean ± standard deviation. Comparisons between groups were made using ordinary one-way analysis of variance with GraphPad Prism 8.0.1 software. Statistical significance was set at $P < 0.05$.

RESULTS

Sodium ferulate inhibits NET formation in kidney tissues of MPO-AVV mice

After establishing the mouse model of immune vasculitis, we observed that compared with normal mice, Rag2 KO mice in the MPO-AAV model group showed symptoms, such as decreased activity, listlessness, decreased appetite, weight loss, and dull hair, indicating that MPO-AAV model mice have immune vasculitis. Immunofluorescence staining showed that the ANCA fluorescence of MPO-AVV mice was greatly enhanced [Figure 1a and b], indicating the successful establishment of the MPO-AAV model. Subsequently, our results showed that after the mice were treated with sodium ferulate by gavage, the ANCA fluorescence in the sodium ferulate group decreased but remained considerably higher than that in the control group [Figure 1a and b]. Fluorescence detection results indicated that NETs in the MPO-AVV mice increased considerably compared with those in the control, and the fluorescence intensity of H3Cit and MPO increased remarkably. NET network formation was observed in the micrographs of MPO-AVV mice. Following gavage treatment with sodium ferulate, a decrease in NETs was observed, along with a reduction in the fluorescence intensity of H3Cit and MPO, compared to MPO-AVV mice [Figure 1c-f].

Sodium ferulate inhibits platelet activation in MPO-AVV mice

CD62p and PAC-1 are markers of platelet activation. In this experiment, we used flow cytometry to determine the number of activated platelets in mice. As shown in Figure 2a-d, the CD62p- and PAC-1-positive cells in the model group increased dramatically, and the magnitude of platelet activation in the model group increased. After sodium ferulate treatment, the number of CD62p- and PAC-1-positive cells decreased, whereas the level of platelet activation in the cells decreased. Meanwhile, the concentrations of β-TG and PAF in the serum samples were measured using ELISA. β-TG is an active substance released after platelet activation, and PAF can induce platelet activation. The results showed that the concentrations of β-TG and PAF in the serum samples greatly increased in the model compared with the control. In the sodium ferulate-treated group, the concentrations of β-TG and PAF were significantly lower than those in the model group [Figure 2e and f]. Meanwhile, the assay of platelet thrombin generation time showed [Figure 2g] that the generation time in the model group was much lower than that in the control group. After sodium ferulate treatment, platelet thrombin generation time was recovered partially but still lower than that in the control group.

Sodium ferulate alleviates endothelial function damage of MPO-AVV mice

Furthermore, the expression levels of PAC-1 and β-TG in the renal tissue were determined by qPCR and Western blot, and the activation status of platelets was evaluated. The expression levels of sTM, iNOS, and TNF-α were measured to study the effect of sodium ferulate on endothelial damage. Consistent with the above results, as illustrated in Figures 3a-e and 4a-f, compared with the control, the gene and protein content of PAC-1 and β-TG in the kidney tissue of immune vasculitis mice increased, and the level of platelet activation increased. After sodium ferulate was administered by gavage, the expression levels of PAC-1 and β-TG in renal tissue were decreased, and the platelet activation state was inhibited. sTM, iNOS, and TNF-α gene and protein expression levels were greatly enhanced in the model group compared with the control and decreased after sodium ferulate treatment. sTM, iNOS, and TNF-α gene and protein expression levels remained significantly elevated relative to those in the control [Figures 3a-e and 4a-f].

Efficacy of sodium ferulate on EPCs

To explore the efficacy of sodium ferulate in endothelial dysfunction at the cellular level, we used the collected peripheral blood of 30 patients with vasculitis, and EPCs

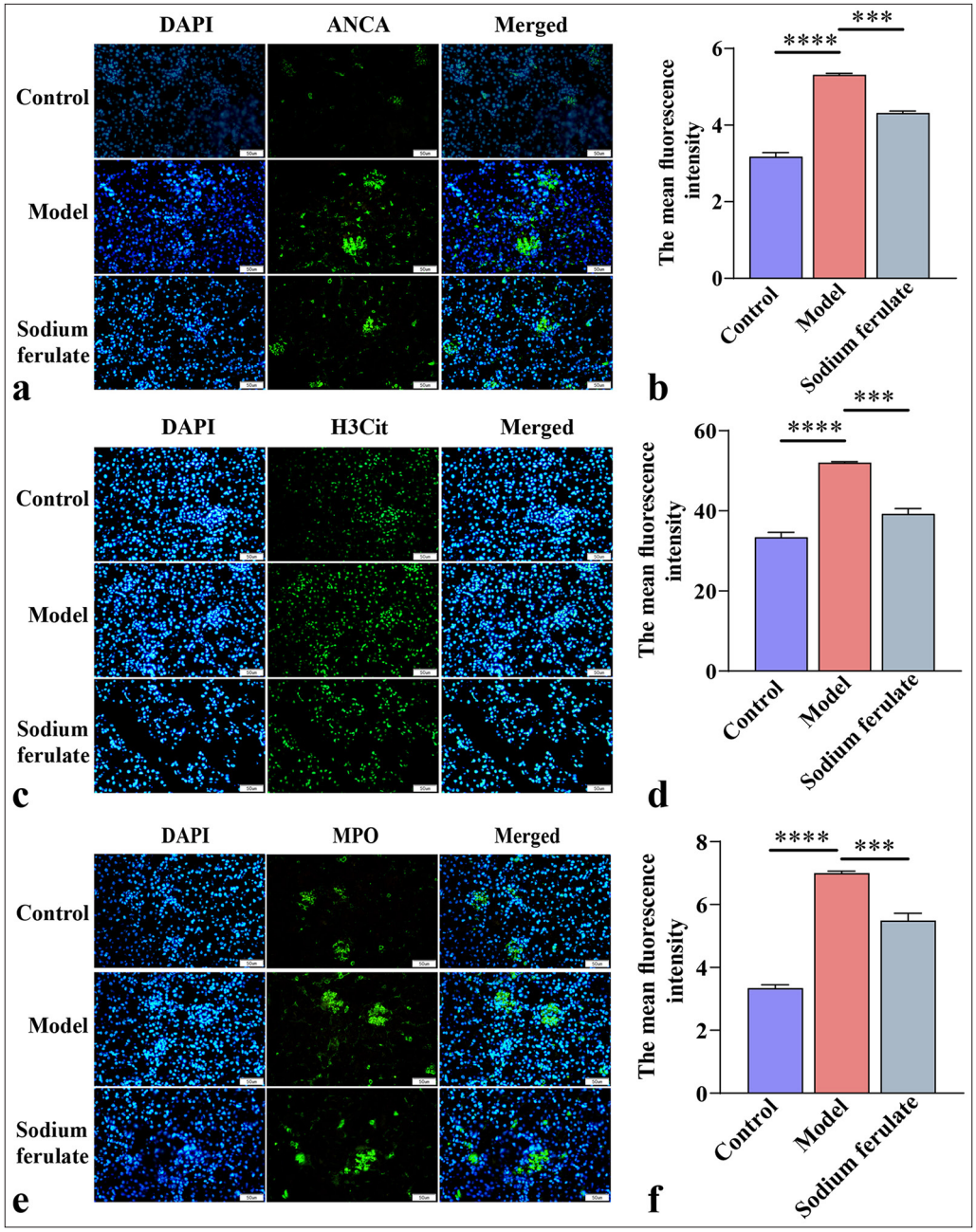

Figure 1: Immunofluorescence microscopy of ANCA, H3Cit, and MPO. (a and b) ANCA immunofluorescence microscopy observation and its average fluorescence intensity; (c and d) H3Cit immunofluorescence microscopy observation and its average fluorescence intensity; (e and f) MPO immunofluorescence microscopy observation and its average fluorescence intensity at original magnification (×400). Scale bar = 50 μm. Data of three independent experiments are presented as mean ± SD and subjected to ordinary one-way ANOVA ("***" indicates statistically significant difference at $P < 0.001$, and "****" indicates extremely significant difference at $P < 0.0001$. DAPI: 4′,6-Diamidino-2-phenylindole, H3Cit: Histone H3 citrullinated, ANCA: Antineutrophil cytoplasmic antibody, MPO: Myeloperoxidase, ANOVA: Analysis of variance).

from the peripheral blood were obtained by density gradient centrifugation and cultured. The resulting EPCs were identified and detected for mycoplasma infection, which showed no mycoplasma infection. The cultured cells were stimulated at different serum concentrations, and the effect on the endothelial function of different groups was

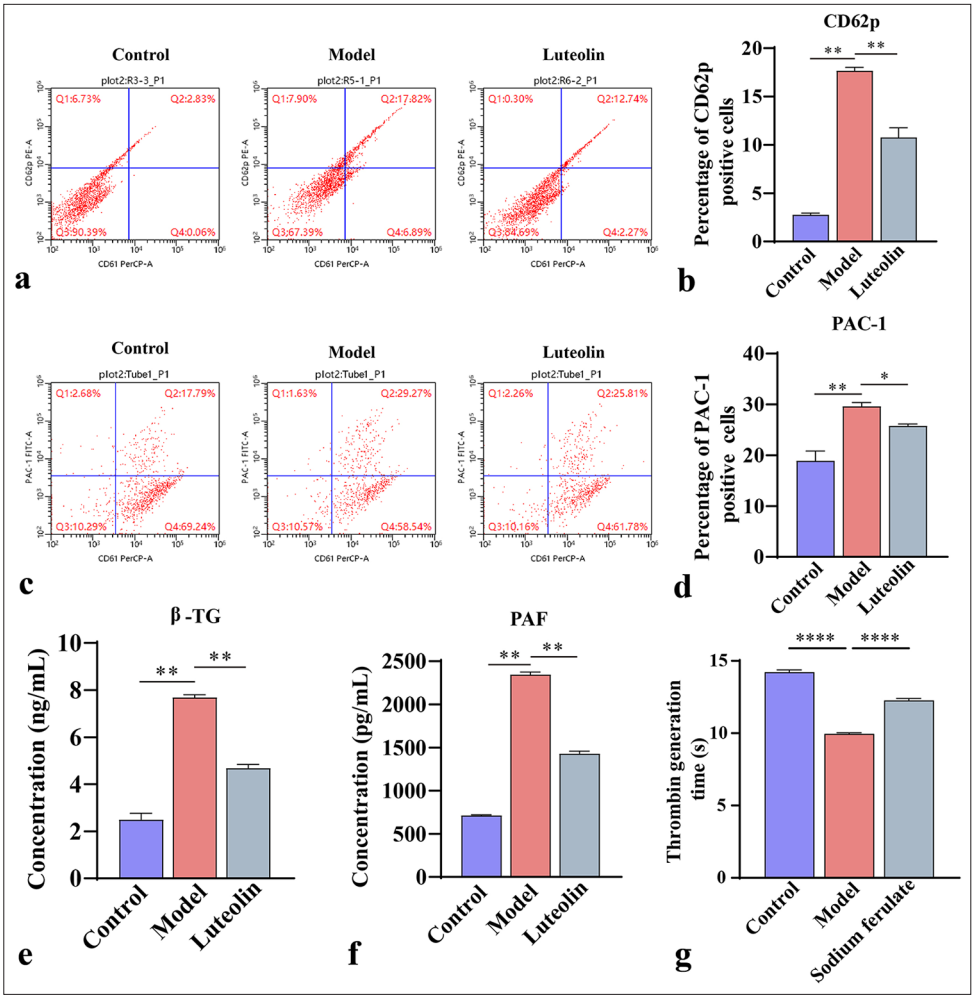

Figure 2: Platelet activation assessment. (a and b) CD62p, a biomarker of platelet activation, and its percentage of positive cells by flow cytometry; (c and d) PAC-1 B, a biomarker of platelet activation, and its percentage of positive cells by flow cytometry; (e and f) Enzyme-linked immunosorbent assay for β-TG and PAF concentrations in mouse serum; (g) Platelet thrombin generation time was measured by thrombin generation assay. Data of three independent experiments are presented as mean ± SD and subjected to ordinary one-way ANOVA ("*" indicates a statistically significant difference at $P < 0.05$, "**" indicates a statistically significant difference at $P < 0.01$, and "****" indicates extremely significant difference at $P < 0.0001$. CD62P: Platelet-selectin, β-TG: β-Trace protein, PAC-1: Procaspase-activating compound-1, PAF: Platelet-activating factor, ANOVA: Analysis of variance, SD: Standard deviation).

determined. Similarly, in the model group, the release of NETs in EPCs treated with serum samples from patients with vasculitis considerably increased, and sodium ferulate suppressed the release of NETs in a concentration-dependent manner. As the concentration of sodium ferulate increased, the inhibitory effect improved [Figure 5a]. The MTT assay was used in determining the survival rate of the EPCs, and the findings indicated that sodium ferulate ameliorated the cell survival rate of EPCs, in contrast to the model [Figure 5b]. The ultrastructure of EPCs was observed by transmission electron microscopy, and the images displayed in [Figure 5c] show that different degrees of mitochondrial swelling and endoplasmic reticulum expansion existed in the groups compared with the control. The concentrations of PAC-1, β-TG, and iNOS in the model were substantially increased but decreased after sodium ferulate treatment, showing a dose-dependent response to the concentration of sodium ferulate [Figure 6a-c]. vWF, β-TG, and iNOS protein expression in the tissue was determined by western blotting, as illustrated in [Figure 6d and e]. Compared with the control group, the protein expression of vWF, β-TG, and iNOS was observed in the model group, and sodium ferulate reduced the expression of vWF, β-TG, and iNOS protein in the tissues.

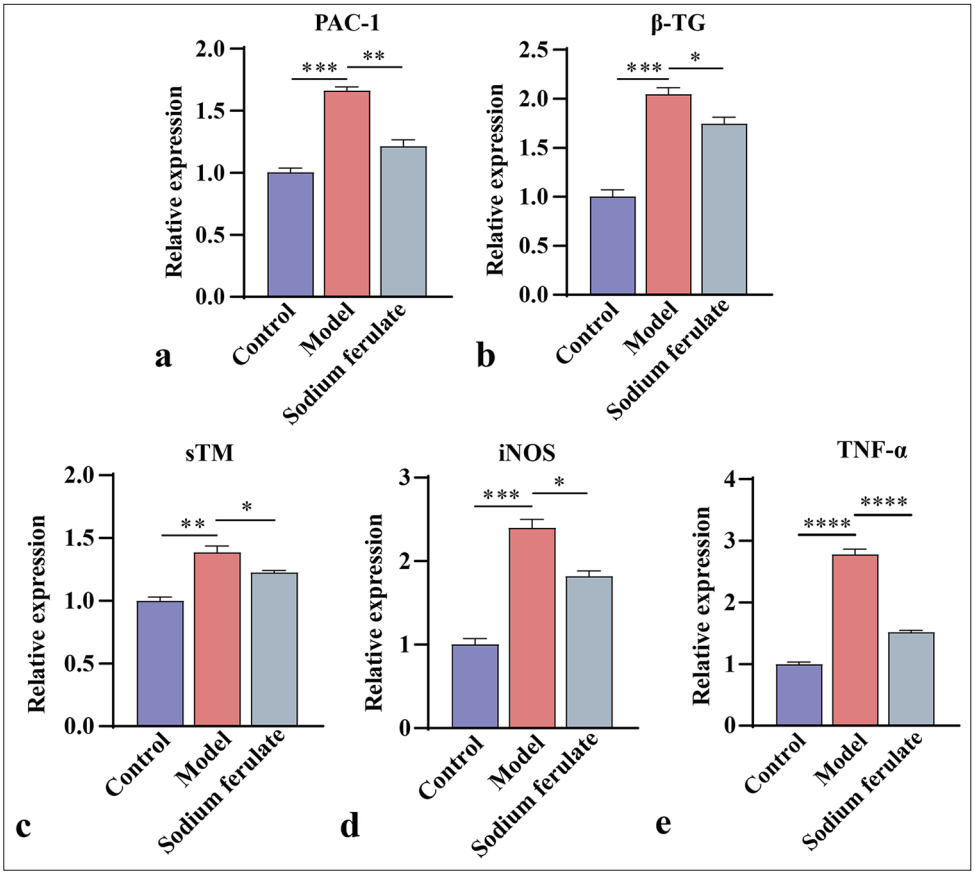

Figure 3: Efficacy of sodium ferulate in affecting PAC-1, β-TG, sTM, iNOS, and TNF-α content in the kidney tissues of MPO-AAV mice. (a) Relative mRNA gene level of *PAC-1*; (b) relative mRNA gene level of *β-TG*; (c) relative mRNA gene level of *sTM*; (d) relative mRNA gene level of *iNOS*; (e) relative mRNA gene level of *TNF-α*. Data of three independent experiments are presented as mean ± SD and subjected to ordinary one-way ANOVA ("*" indicates a statistically significant difference at $P < 0.05$, "**" indicates a statistically significant difference at $P < 0.01$, "***" indicates statistically significant difference at $P < 0.001$ and "****" indicates extremely significant difference at $P < 0.0001$. PAC-1: Procaspase-activating compound-1, β-TG: β-Trace protein, sTM: Soluble thrombomodulin, iNOS: Inducible nitric oxide synthase, TNF-α: Tumor necrosis factor α, MPO: Myeloperoxidase, AAV: Associated vasculitis, mRNA: Messenger ribonucleic acid, ANOVA: Analysis of variance, SD: Standard deviation).

DISCUSSION

The pathogenesis of AAV is still unclear, but the current research suggests that it is related to infection, drugs, environment, and genetic factors.[21,22] Epidemiology demonstrates significant geographic and age differences. ANCA-associated small vessel vasculitis is common in China but has a low diagnosis rate and poor overall prognosis.[23] The correlation between age and prognosis of ANCA-associated small-vessel vasculitis, which mainly occurs in patients aged > 65 years old,[24] was explored in this study. Routine treatment of the disease is required for old patients, although the use of hormones can control the development of the disease. Old patients have poor hormone tolerance and adverse reactions to immunosuppressants, and deficiencies are present.[25]

We first established the MPO-AAV mouse vasculitis model, detected the release of NETs and platelet activation state, and studied the therapeutic effect of sodium ferulate on mouse vasculitis and the effect of endothelial function damage in mice. The results showed that sodium ferulate can significantly reduce the expression of ANCA protein in MPO-AAV mice, inhibit the release of NETs in renal tissues, and reduce the expression of NET markers H3Cit and MPO in renal tissues.[26] NETs can capture and kill pathogenic microorganisms; however, excessive NET formation can promote tissue and organ damage. NETs are deposited in the damaged parts of the renal tissues in patients.[27] ANCA can bind to MPO on the surfaces of neutrophils activated by pro-inflammatory factors, leading to increased neutrophil activation and the release of NETs and aggravating the

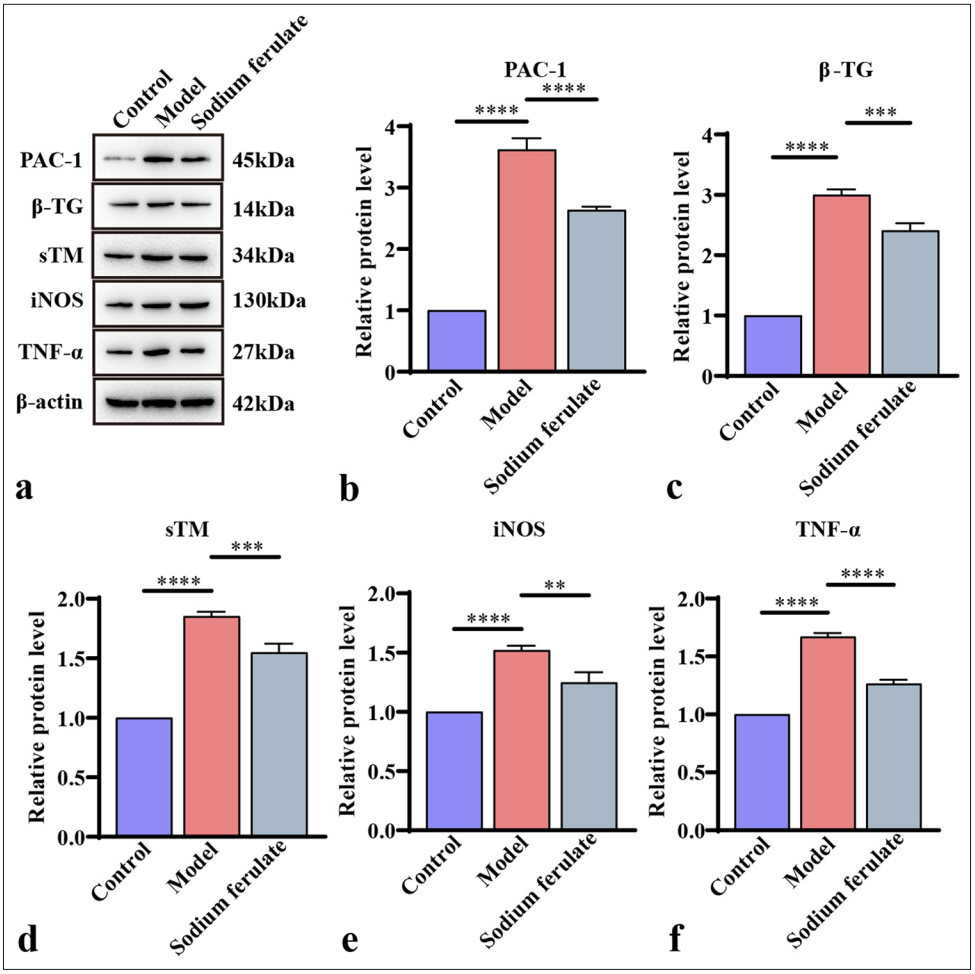

Figure 4: Efficacy of sodium ferulate in affecting content of PAC-1, β-TG, sTM, iNOS, and TNF-α in the kidney tissues of MPO-AAV mice. (a) Western blot detection of the protein bands of PAC-1, β-TG, sTM, iNOS, and TNF-α; (b) grayscale analysis of PAC-1 bands; (c) grayscale analysis of β-TG bands; (d) grayscale analysis of sTM bands; (e) grayscale analysis of iNOS bands; (f) grayscale analysis of TNF-α bands. Data of three independent experiments are presented as mean ± SD and subjected to ordinary one-way ANOVA ("**" indicates a statistically significant difference at $P < 0.01$, "***" indicates a highly significant difference at $P < 0.001$, and "****" indicates extremely significant difference at $P < 0.0001$. PAC-1: Procaspase-activating compound-1, β-TG: β-Trace protein, sTM: Soluble thrombomodulin, iNOS: Inducible nitric oxide synthase, TNF-α: Tumor necrosis factor-α, MPO: Myeloperoxidase, AAV: Associated vasculitis, ANOVA: Analysis of variance, SD: Standard deviation).

pathological process of AAV. In addition, sodium ferulate inhibited cellular platelet activation and decreased the number of CD62p- and PAC-1-positive cells and serum β-TG and PAF concentrations. Platelets act as immune cells by phagocytosing microorganisms, which not only have hemostatic functions but also induce inflammation,[28] participate in innate and adaptive immune responses, and mediate vascular inflammatory injury, which is pivotal to the progression of AAV.[29-32] The TNF (ligand) superfamily member 5 (CD154) can exist in platelets, and when platelets are activated, CD154 molecules can be released.[33] Platelet-related CD154 interacts with CD40 antigen (CD40) on the surface of endothelial cells and upregulates the expression of intercellular cell adhesion molecule-1 (ICAM-1) and C-C motif chemokine ligand 2, thereby inducing leukocyte chemotaxis and endothelial cell damage[34] and then mediating vascular inflammation change.

We evaluated the effect of sodium ferulate on NET-platelet activation-mediated endothelial dysfunction in mice by measuring the expression levels of sTM, iNOS, and TNF-α. sTM is a sensitive and specific molecular marker for endothelial injury. iNOS can be induced by various stimuli and is expressed in large quantities. It catalyzes excessive

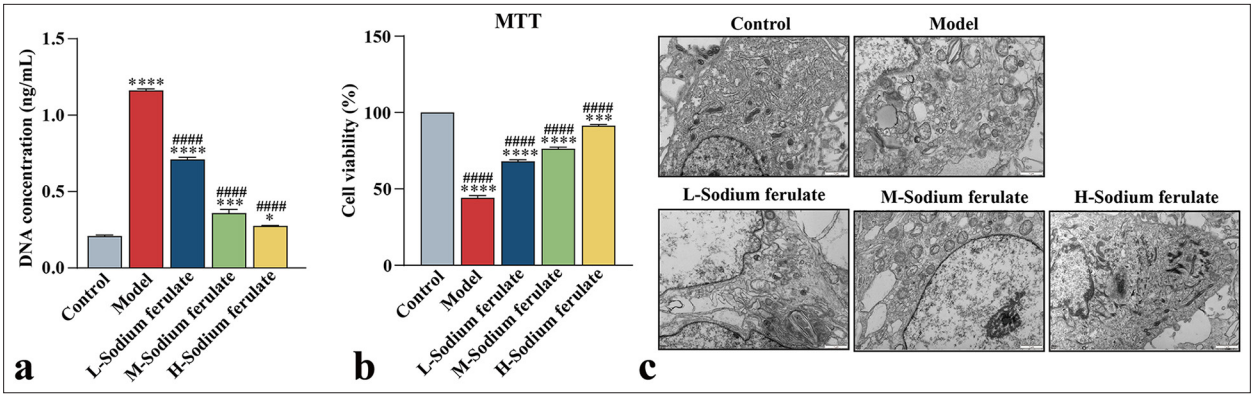

Figure 5: Effect of sodium ferulate on serum stimulated EPCs. (a) Detection of NETs by fluorescence staining; (b) MTT assay to assess the viability of EPCs; (c) ultrastructure of serum-stimulated EPCs by transmission electron microscopy, where "L-sodium ferulate" denotes low-dose sodium ferulate, "M-sodium ferulate" denotes medium-dose sodium ferulate, and "H-sodium ferulate" denotes high-dose sodium ferulate. MTT: 3-(4,5-Dimethylthiazol-2-yl)-2,5-diphenyltetrazolium bromide assay, EPCs: Endothelial progenitor cells, NETs: neutrophil extracellular traps. Scale bar = 1 μm. Data of three independent experiments are presented as mean ± SD and subjected to ordinary one-way ANOVA (Significance was represented by asterisks: *, $P < 0.05$, ***, $P < 0.001$, ****, $P < 0.0001$ versus control. ####, $P < 0.0001$ versus model, ANOVA: Analysis of variance, SD: Standard deviation).

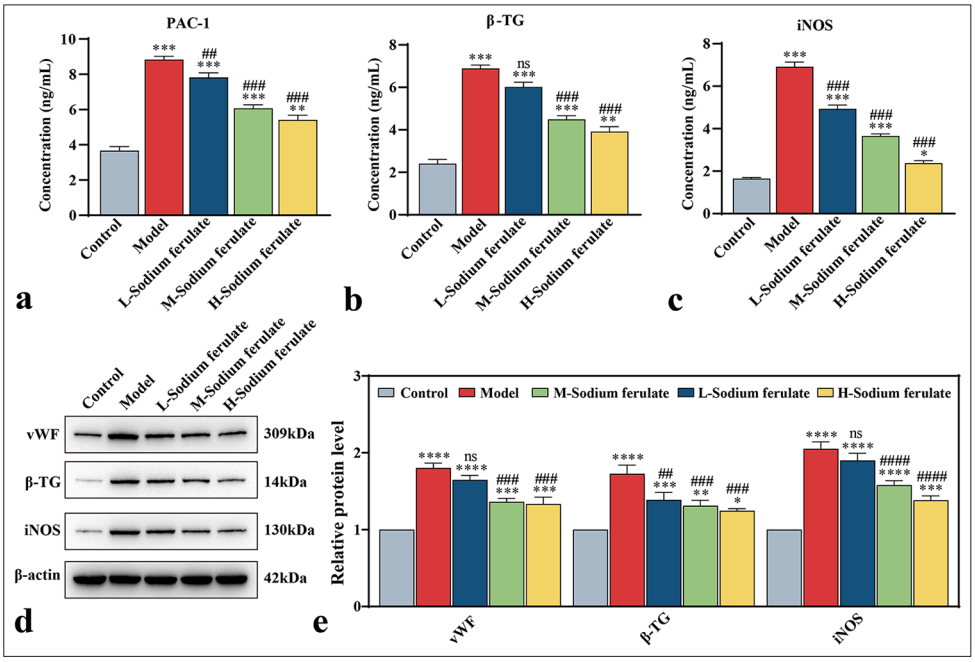

Figure 6: Effect of sodium ferulate on serum stimulated EPCs. (a) Concentration of PAC-1 in the supernatant of stimulated EPCs; (b) concentration of β-TG in the supernatant of stimulated EPCs; (c) concentration of iNOS in the supernatant of stimulated EPCs; (d) Western blotting to detect the protein bands of vWF, β-TG, and iNOS; (e) analysis of the gray values of the protein bands of vWF, β-TG, and iNOS. Relative analysis was made based on the gray value of the strip chart; β-actin employed as the endogenous control, where "L-sodium ferulate" denotes low-dose sodium ferulate, "M-sodium ferulate" denotes medium-dose sodium ferulate, and "H-sodium ferulate" denotes high-dose sodium ferulate. Data of three independent experiments are presented as mean ± SD and subjected to ordinary one-way ANOVA.Significance is indicated by asterisks: *, $P < 0.05$, **, $P < 0.01$; ***, $P < 0.001$, ****, $P < 0.0001$ compared with the control. "ns" indicates no statistical significance compared with the model, ##, $P < 0.01$ ###, $P < 0.001$, ####, $P < 0.0001$ versus model (PAC-1: Procaspase-activating compound-1, β-TG: β-Trace protein, iNOS: Inducible nitric oxide synthase, vWF: von Willebrand Factor, ANOVA: Analysis of variance, EPCs: Endothelial progenitor cells, SD: Standard deviation).

NO production, participates in oxidative stress, and causes vascular endothelial injury.[35] As a pro-inflammatory cytokine, TNF-α plays various physiological and pathological roles in cellular immune responses. Vascular endothelial cells can be activated by TNF-α and then express many cytokines and adhesion molecules that initiate consecutive inflammatory leukocyte infiltration and inflammatory reactions. The findings demonstrated that the protein and gene expression of sTM, iNOS, and TNF-α were dramatically increased in MPO-AAV mice compared with normal controls, and the protein and gene expression levels decreased after sodium ferulate treatment. These results suggest that sodium ferulate is a potential therapeutic agent for AAV. Notably, Shen *et al*. indicated that the combination therapy with sodium ferulate can improve clinical efficacy in patients with coronary heart disease and can positively affect electrocardiography efficacy, frequency of angina attacks, endothelium-dependent flow-mediated vasodilation, nitric oxide, endothelin, whole blood low shear rate, platelet aggregation test, C-reactive protein, TNF-α, interleukin-6, and triglyceride level.[19]

Subsequently, we isolated and cultured EPCs and treated the cells with different concentrations of sodium ferulate. Our findings provide clear evidence that the release of NETs in EPCs exposed to sera from patients with vasculitis considerably increased. This effect was accompanied by a decrease in cell survival rate and evident pathological swelling in the ultrastructural configuration of the cells. Conversely, sodium ferulate impeded NET release and mitigated EPC cellular damage. Moreover, sodium ferulate reduced the expression of vWF, β-TG, and iNOS proteins in the tissues. vWF is often released after vascular endothelial injury and is accompanied by the enhanced expression of ICAM-1 and vascular cell adhesion molecule 1, which can be used as markers of vascular endothelial cell injury.[36] This study has limitations. First, the study was limited in scope, focusing exclusively on the impact of sodium ferulate on endothelial function impairment resulting from NET-platelet activation in the MPO-AAV model. The findings of the present study did not encompass other AAV models or clinical trials, and thus, the generalizability of the findings to other AAV patient populations remains to be established. Second, the study only observed the inhibitory effect of sodium ferulate on NET release, platelet activation, and endothelial damage. The molecular mechanism underlying this effect was not investigated. That is, whether sodium ferulate acts directly on neutrophils or through other pathways were not determined, and the specific target of action was not identified. Further exploration of these aspects is necessary. Ultimately, the study concentrated on the therapeutic efficacy of sodium ferulate for AAV, but the pharmacological characteristics of the drug, including the optimal dosage, route of administration, safety profile, and other aspects, require further investigation.

SUMMARY

Sodium ferulate can attenuate endothelial function injury mediated by NET-platelet activation in AAV *in vivo* and *in vitro*. An alternative therapy for AAV was proposed, and the results offer valuable insights into the role of sodium ferulate in AAV treatment.

AVAILABILITY OF DATA AND MATERIALS

The data that support the findings of this study are available from the corresponding author, upon reasonable request.

ABBREVIATIONS

AAV: Anti-neutrophil cytoplasmic antibody-associated vasculitis
ANCA: Anti-neutrophil cytoplasmic antibody
CD62p: Platelet-selectin
CO_2: Carbon dioxide
ELISA: Enzyme-linked immunosorbent assay
EPCs: Endothelial progenitor cells
H3Cit: Histone H3 citrullinated
IgG: Immunoglobulin G
iNOS: Inducible nitric oxide synthase
MPO: Myeloperoxidase
MTT: 3-(4,5-Dimethylthiazol-2-yl)-2,5-diphenyltetrazolium bromide
NETs: Neutrophil extracellular traps
PAC-1: Procaspase-activating compound-1
PAF: Platelet-activating factor
PBMCs: Peripheral blood mononuclear cells
PBS: Phosphate-buffered saline
PR3: Proteinase 3
qPCR: Real-time quantitative polymerase chain reaction
Rag2 KO: Recombination activating gene 2 knockout
RNA: Ribonucleic acid
SPF: Specific pathogen-free
sTM: Soluble thrombomodulin
TNF-α: Tumor necrosis factor α
vWF: von Willebrand Factor
β-TG: β-Trace protein

AUTHOR CONTRIBUTIONS

XLZ and ZJW: Participated in the conception of this study and review the manuscript; ZJW, WXL and QLY: Performed the experiments, analyzed the data, and wrote the manuscript; CX and YHZ: Helped with the data analysis; and WP: Provided constructive discussions. All authors have read and approved the final version of the forthcoming article.

ETHICS APPROVAL AND CONSENT TO PARTICIPATE

All experiments involving human patients in our study followed the ethical regulations of the Ethics Committee of Chongqing Traditional Chinese Medicine Hospital and have been approved by the Committee (Ethics Approval No. 2020-ky-64, Chongqing Hospital of Traditional Chinese Medicine; Approval Date: January 25, 2021). We ensured the rights and interests of all participants and obtained their informed consent. In addition, the study strictly followed the experimental animal management methods approved by the Ethics Committee of Chongqing Traditional Chinese Medicine Hospital (Approval No. 2022-DWSY-ZXL; Approval Date: November 7, 2022). We followed strict animal welfare standards and ensured animal comfort and minimized suffering during the experiments. Finally, we are committed that all aspects of the study followed the ethical principles of the Declaration of Helsinki. Informed consent was obtained from all participants for all experiments in this study after the nature and potential risks of the study were explained to them. They were also informed of their right to withdraw from the study at any time without penalty.

ACKNOWLEDGMENT

Not applicable.

FUNDING

This study was sponsored by the General Project of Chongqing Natural Science Foundation (No. cstc2020jcyj-msxmX1018). The Fifth Batch of National Traditional Chinese Medicine Excellent Clinical Talents Training Project. (Announcement from the Personnel and Education Department of the National Administration of Traditional Chinese Medicine. No. 2022-1).

CONFLICT OF INTEREST

The authors declare no conflict of interest.

EDITORIAL/PEER REVIEW

To ensure the integrity and highest quality of CytoJournal publications, the review process of this manuscript was conducted under a **double-blind model** (authors are blinded for reviewers and vice versa) through an automatic online system.

REFERENCES

1. Nakazawa D, Masuda S, Tomaru U, Ishizu A. Pathogenesis and therapeutic interventions for ANCA-associated vasculitis. Nat Rev Rheumatol 2019;15:91-101.
2. Kitching AR, Anders HJ, Basu N, Brouwer E, Gordon J, Jayne DR, *et al*. ANCA-associated vasculitis. Nat Rev Dis Primers 2020;6:71.
3. Guchelaar NA, Waling MM, Adhin AA, van Daele PL, Schreurs MW, Rombach SM. The value of anti-neutrophil cytoplasmic antibodies (ANCA) testing for the diagnosis of ANCA-associated vasculitis, a systematic review and meta-analysis. Autoimmun Rev 2021;20:102716.
4. Ríos-López AL, González GM, Hernández-Bello R, Sánchez-González A. Avoiding the trap: Mechanisms developed by pathogens to escape neutrophil extracellular traps. Microbiol Res 2021;243:126644.
5. Liu L, Mao Y, Xu B, Zhang X, Fang C, Ma Y, *et al*. Induction of neutrophil extracellular traps during tissue injury: Involvement of STING and Toll-like receptor 9 pathways. Cell Prolif 2019;52:e12579.
6. Papayannopoulos V. Neutrophil extracellular traps in immunity and disease. Nat Rev Immunol 2018;18:134-47.
7. Mutua V, Gershwin LJ. A review of neutrophil extracellular traps (NETs) in disease: Potential anti-NETs therapeutics. Clin Rev Allergy Immunol 2021;61:194-211.
8. Li RH, Tablin F. A comparative review of neutrophil extracellular traps in sepsis. Front Vet Sci 2018;5:291.
9. Glennon-Alty L, Hackett AP, Chapman EA, Wright HL. Neutrophils and redox stress in the pathogenesis of autoimmune disease. Free Radic Biol Med 2018;125:25-35.
10. Griffiths CE, Armstrong AW, Gudjonsson JE, Barker J. Psoriasis. Lancet 2021;397:1301-15.
11. Siegel CH, Sammaritano LR. Systemic lupus erythematosus: A review. JAMA 2024;331:1480-91.
12. Wigerblad G, Kaplan MJ. NETs spread ever wider in rheumatic diseases. Nat Rev Rheumatol 2020;16:73-4.
13. Nishibata Y, Arai S, Taniguchi M, Nakade I, Ogawa H, Kitano S, *et al*. Cathepsin C inhibition reduces neutrophil serine protease activity and improves activated neutrophil-mediated disorders. Nat Commun 2024;15:6519.
14. Rogler G, Singh A, Kavanaugh A, Rubin DT. Extraintestinal manifestations of inflammatory bowel disease: Current concepts, treatment, and implications for disease management. Gastroenterology 2021;161:1118-32.
15. Asemota U, Greenberg S, Gulati A, Kumar K, Janga K. Tofacitinib-induced antineutrophil cytoplasmic antibodies (ANCA)-associated vasculitis with crescentic glomerulonephritis. Cureus 2021;13:e18663.
16. Bai YH, Li ZY, Chang DY, Chen M, Kallenberg CG, Zhao MH. The BVAS is an independent predictor of cardiovascular events and cardiovascular disease-related mortality in patients with ANCA-associated vasculitis: A study of 504 cases in a single Chinese center. Semin Arthritis Rheum 2018;47:524-9.
17. Guo W, Li Y, An D, Zhou M, Xiong J, Jiang Z, *et al*. Sodium ferulate-functionalized silver nanopyramides with synergistic antithrombotic activity for thromboprophylaxis. Colloids Surf B Biointerfaces 2022;220:112925.
18. Xue R, Fan XL, Yang Q, Yu C, Lu TY, Wan GM. Protective effect of ethyl ferulate against hypoxic injury in retinal cells and retinal neovascularization in an oxygen-induced retinopathy model. Phytomedicine 2023;121:155097.
19. Shen Z, Wu Y, Zhou L, Wang Q, Tang Y, Sun Y, *et al*. The efficacy

of sodium ferulate combination therapy in coronary heart disease: A systematic review and meta-analysis. Phytomedicine 2023;115:154829.
20. Hu P, Su H, Xiao H, Gou SJ, Herrera CA, Alba MA, *et al.* Kinin B1 receptor is important in the pathogenesis of myeloperoxidase-specific ANCA GN. J Am Soc Nephrol 2020;31:297-307.
21. Trivioli G, Marquez A, Martorana D, Tesi M, Kronbichler A, Lyons PA, *et al.* Genetics of ANCA-associated vasculitis: Role in pathogenesis, classification and management. Nat Rev Rheumatol 2022;18:559-74.
22. Casal Moura M, Gauckler P, Anders HJ, Bruchfeld A, Fernandez-Juarez GM, Floege J, *et al.* Management of antineutrophil cytoplasmic antibody-associated vasculitis with glomerulonephritis as proposed by the ACR 2021, EULAR 2022 and KDIGO 2021 guidelines/recommendations. Nephrol Dial Transplant 2023;38:2637-51.
23. Centenera MM, Scott JS, Machiels J, Nassar ZD, Miller DC, Zinonos I, *et al.* ELOVL5 is a critical and targetable fatty acid elongase in prostate cancer. Cancer Res 2021;81:1704-18.
24. Xiapei F, Liangliang C, Binfeng Y, Yanhong M, Ying X, Jianghua C, *et al.* Pathological classification and prognosis of renal damage caused by antineutrophil cytoplasmic antibody associated vasculitis. Chin J Nephrol 2019;35:88-93.
25. Qi G, Lin Y. Clinical analysis of 4 1 cases of antineutrophil cytoplasmic antibody assoiated vasculitis. J Clin Nephrol 2018;18:348-52.
26. Nomura K, Miyashita T, Yamamoto Y, Munesue S, Harashima A, Takayama H, *et al.* Citrullinated histone H3: Early biomarker of neutrophil extracellular traps in septic liver damage. J Surg Res 2019;234:132-8.
27. Demkow U. Molecular mechanisms of neutrophil extracellular trap (NETs) degradation. Int J Mol Sci 2023;24:4896.
28. Li S, Lu Z, Wu S, Chu T, Li B, Qi F, *et al.* The dynamic role of platelets in cancer progression and their therapeutic implications. Nat Rev Cancer 2024;24:72-87.
29. Salabarria SM, Corti M, Coleman KE, Wichman MB, Berthy JA, D'Souza P, *et al.* Thrombotic microangiopathy following systemic AAV administration is dependent on anti-capsid antibodies. J Clin Invest 2024;134:e173510.
30. Sun XJ, Li ZY, Chen M. Pathogenesis of anti-neutrophil cytoplasmic antibody-associated vasculitis. Rheumatol Immunol Res 2023;4:11-21.
31. Baier E, Tampe D, Kluge IA, Hakroush S, Tampe B. Implication of platelets and complement C3 as link between innate immunity and tubulointerstitial injury in renal vasculitis with MPO-ANCA seropositivity. Front Immunol 2022;13:1054457.
32. Matsumoto K, Yasuoka H, Yoshimoto K, Suzuki K, Takeuchi T. Platelet CXCL4 mediates neutrophil extracellular traps formation in ANCA-associated vasculitis. Sci Rep 2021;11:222.
33. Hassan GS, Salti S, Mourad W. Novel functions of integrins as receptors of CD154: Their role in inflammation and apoptosis. Cells 2022;11:1747.
34. Koupenova M, Livada AC, Morrell CN. Platelet and megakaryocyte roles in innate and adaptive immunity. Circ Res 2022;130:288-308.
35. Li D, Rui YX, Guo SD, Luan F, Liu R, Zeng N. Ferulic acid: A review of its pharmacology, pharmacokinetics and derivatives. Life Sci 2021;284:119921.
36. Huang X, Zhang X, Machireddy N, Evans CE, Trewartha SD, Hu G, *et al.* Endothelial FoxM1 reactivates aging-impaired endothelial regeneration for vascular repair and resolution of inflammatory lung injury. Sci Transl Med 2023;15:eabm5755.

How to cite this article: Zhou X, Wang Z, Liao W, Yin Q, Xiong C, Zheng Y, *et al.* Influence of sodium ferulate on neutrophil extracellular traps-platelet activation-mediated endothelial dysfunction in immune small vasculitis. CytoJournal. 2024;21:76. doi: 10.25259/Cytojournal_153_2024

HTML *of this article is available FREE at:*
https://dx.doi.org/10.25259/Cytojournal_153_2024